Naval Research Laboratory

Washington, DC 20375-5320

AD-A281 014

NRL/MR/7220--94-7478

Using Lidar Tomography to Characterize Scattering in a Turbulent Media

WILLIAM P. HOOPER

Remote Sensing Physics Branch
Remote Sensing Division

March 28, 1994

DTIC
ELECTE
JUL 06 1994
S
G
D

DTIC QUALITY INSPECTED 3

94-20467

94 7 5 182

REPORT DOCUMENTATION PAGE

Form Approved
OMB No. 0704-0188

1. AGENCY USE ONLY (Leave Blank)	2. REPORT DATE	3. REPORT TYPE AND DATES COVERED
	March 28, 1994	

4. TITLE AND SUBTITLE	5. FUNDING NUMBERS
Using Lidar Tomography to Characterize Scattering in a Turbulent Media	PE - 61153N
6. AUTHOR(S)	PR - RR0310341
William P. Hooper	WU - 321400

7. PERFORMING ORGANIZATION NAME(S) AND ADDRESS(ES)	8. PERFORMING ORGANIZATION REPORT NUMBER
Naval Research Laboratory Washington, DC 20375-5320	NRL/MR/7220--94-7478

9. SPONSORING/MONITORING AGENCY NAME(S) AND ADDRESS(ES)	10. SPONSORING/MONITORING AGENCY REPORT NUMBER
Office of Naval Research Arlington, VA 22217-5660	

11. SUPPLEMENTARY NOTES

12a. DISTRIBUTION/AVAILABILITY STATEMENT	12b. DISTRIBUTION CODE
Approved for public release; distribution unlimited.	

13. ABSTRACT (Maximum 200 words)

A tomographic method for objectively determining extinction and backscatter using a single, scanning wavelength lidar is outlined. In the theoretical analysis, the scattering media is observed from different directions by a lidar which is either moved or observes the structures as they drift past the lidar. A matrix equation is developed and tested by randomly selecting extinction and backscatter values on a 5 by 5 grid. Measurement and turbulence induced errors are modeled and the measurement accuracies are assessed. Results for the theoretical calculations suggest that the method would provide accurate results for a scanning airborne lidar, but not from a scanning system that does not move.

14. SUBJECT TERMS			15. NUMBER OF PAGES
Lidar	Laser radar		15
Tomography	Extinction		**16. PRICE CODE**
Aerosol			

17. SECURITY CLASSIFICATION OF REPORT	18. SECURITY CLASSIFICATION OF THIS PAGE	19. SECURITY CLASSIFICATION OF ABSTRACT	20. LIMITATION OF ABSTRACT
UNCLASSIFIED	UNCLASSIFIED	UNCLASSIFIED	UL

CONTENTS

Accesion For

NTIS CRA&I	☒
DTIC TAB	☐
Unannounced	☐
Justification	

By _____

Distribution /

Availability Codes

| Dist | Avail and / or Special |
| A-1 | |

iii

USING LIDAR TOMOGRAPHY TO CHARACTERIZE
IN A TURBULENT MEDIA

1. Introduction

Atmospheric lidar returns depend on both backscatter(β) and extinction(σ)[1]:

$$P(r) = \frac{K\beta(r)}{r^2} \exp\left[-2 \int_{r'=0}^{r} \sigma(r')\,dr'\right], \qquad (1)$$

where P is the power return, r is range, and K contains system constants. Exact determination of extinction and backscatter from a single return requires a knowledge of the range dependence of either extinction or backscatter or the relationship between these variables. However, for multiple returns[2], tomography methods can be used to independently determine extinction and backscatter. In one approach, the logarithmic form of the lidar equation separates the two variables:

$$S(r) = \ln[P(r)r^2/K] = \ln[\beta(r)] - 2\tau(r), \qquad (2)$$

where τ is the optical depth $[\tau(r) = \int_{r'=0}^{r} \sigma(r')\,dr']$ and the lidar data is both range corrected and calibrated. From an aircraft, the lidar can scan 45° forward of vertical, straight down, and 45° aft of vertical, see figure 1:

$$S_{45°} = B_1 - T_1$$
$$S_{0°} = B_2 - T_2 \qquad (3)$$
$$S_{-45°} = B_3 - T_3$$

where B and T are respectively the logarithm backscatter $[\ln[\beta]]$ and twice the optical depth $[2\tau]$.
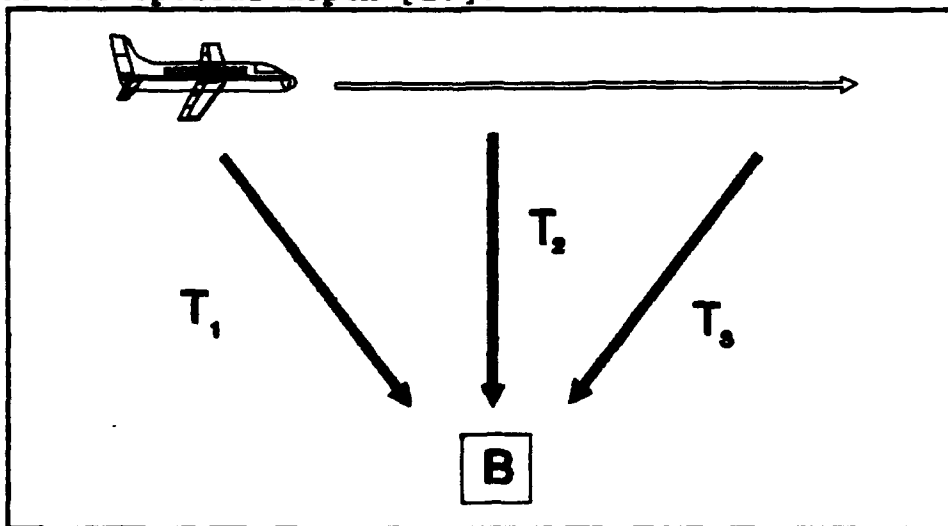
Figure 1. An aircraft flying from left to right makes three tomographic lidar observations of the same volume.

Controlled scanning allows the backscatter at the one point to be observed several times. In a homogeneous atmosphere, the system of equations becomes over-determined:

$$T_1 = T_3 = \frac{T_2}{\cos(45°)}$$

$$B_1 = B_2 = B_3$$

(4)

and the backscatter and extinction can be determined from a set of equations that use a least square fitting process to minimize the errors.

While equations(3) and (4) are overly simplistic, they illuminate the advantage -- over-determined equations -- and limitation of lidar tomography -- the need for homogeneity. Spatial homogeneity is needed since the scattering must be almost homogeneous inside the individual grid elements. If tomography can use regions whose scale sizes are an order of magnitude smaller than the size of the dominant atmospheric structures, the approximation can be quite reasonable. Temporal homogeneity is also needed, ie. the atmosphere must not dramatically change between the measurements. Simply stated, the time between the lidar measurements must be substantially faster than the 'half life' of the dominant atmospheric structures.

This report contains an initial discussion of the tomographic method and will not provide a detailed analysis of equipment and/or atmospheric conditions required for this method to work. While possible instrumental configurations include: mobile lidars, multiple fixed lidars, and even single lidars, only a single scanning lidar (either moving or stationary) is modelled. The model used to test the inversion accuracies are selected for simplicity and ability to test a wide range of conditions; however, the model is not based on any specific atmospheric model.

2. Basic Technique and Equations

In the specific tomography method discussed by this report, a grid divides the atmosphere into equal regions. Each region is assumed to have a constant backscatter and extinction. A discrete form of the lidar equation is used:

$$S_k = B_{i+(j-1) \cdot n} - \sum_{i',j'=1,1}^{n,m} A_{k,i'+(j'-1) \cdot n + n \cdot m} \, T_{i'+(j'-1) \cdot n} \, ,$$

(5)

where i and j represent spatial coordinates, k is a unique number assigned to each return, n and m are the maximum size for the coordinates, and $A_{i,j}$ is a geometrical factor. For extinction, $A_{i,j}$ is determined by the distance through the grid element that the kth profile follows. For backscatter, $A_{i,j}$ is either one (if this return is from this region) or zero. A series of measurements of the same grid are made from different locations, systems of equations are formed, and the equations are combined into a matrix

2

relationship:

$$\begin{vmatrix} S_1 \\ S_2 \\ \cdot \\ S_K \end{vmatrix} = \begin{vmatrix} A_{1,1} & A_{1,2} & \cdot & \cdot \\ A_{2,1} & A_{2,2} & \cdot & \cdot \\ \cdot & \cdot & \cdot & \cdot \\ \cdot & \cdot & \cdot & A_{K,2N} \end{vmatrix} \begin{vmatrix} B_1 \\ B_2 \\ \cdot \\ B_N \\ T_1 \\ T_2 \\ \cdot \\ T_N \end{vmatrix} , \qquad (6)$$

where the matrix equation is $\vec{S} = \tilde{A}\vec{B}$, K is the total number of returns, and N is the total number of grid elements [$n*m$].

Table 1 shows the grid that is used for the tomography calculations. Each square is arbitrarily scaled to one on a side. The center of each square is set to be an integer and the edge then becomes an integer plus (or minus) a half. The wide line on the left hand side, which represents the lidar location, has a j coordinate of 0.5 . The first set of observations (or scan) originate at the top [i=0.5] and the other sets of observations are made at 1/2 step intervals [j=0.5,1.0,1.5, etc.]. Backscatter measurement are made at center of each square [ie. (i=1.0,j=1.0), (i=1.0,j=2.0),.... (i=2.0,j=1.0),...].

Table 1: Atmospheric Grid

		Distance [j]					
		1	2	3	4	5	
Distance/ Time [i]	1	1 26	6 31	11 36	16 41	21 46	1
	2	2 27	7 32	12 37	17 42	22 47	2
	3	3 28	8 33	13 38	18 43	23 48	3
	4	4 29	9 34	14 39	19 44	24 49	4
	5	5 30	10 35	15 40	20 45	25 50	5
		1	2	3	4	5	

The top number in each grid element is the matrix number for the backscattering and the bottom number is the matrix number for the extinction.

3

The coefficients for the first two returns are:
[for a lidar located at (i=0.5,j=0.5) and a return from (i=1.0,j=1.0)]

$$S_1 = B_1 - \frac{\sqrt{2}}{2} T_1 \qquad (7)$$

[In the above case, the coefficients $A_{1,1}$ and $A_{2,26}$ are respectively 1.0 and $\frac{\sqrt{2}}{2}$. All other coefficients for this return are zero (ie. $A_{1,L}=0$ where $L \neq 1$ or 26.]
[for a lidar located at (i=0.5,j=0.5) and a return from (i=1.0,j=2.0)]

$$S_2 = B_6 - \frac{\sqrt{10}}{3} T_1 - \frac{\sqrt{10}}{6} T_6 . \qquad (8)$$

[In the above case, the coefficients $A_{2,6}$, $A_{2,26}$, and $A_{2,31}$ are respectively 1.0, $\frac{\sqrt{10}}{3}$, and $\frac{\sqrt{10}}{6}$].

The scan angles are restricted to less than or equal to 45° [ie. the column change (j) is less than or equal to the row change (i)]. This limitation is not necessary and represents a convenient, but arbitrary restriction. For the grid shown in table 1 and, for the scheme discussed above, 195 returns are possible. Since the equations have 50 unknowns, the equation system is over-determined and the least squares determination of the atmospheric parameters (backscatter and optical depth) becomes[3]:

$$\vec{B}^\bullet = (\ddot{A}^T \ddot{A}^{-1} \ddot{A}^T) \vec{S} \qquad (9)$$

where $\vec{B}^\bullet$ denotes the least square estimate, $\ddot{A}^T$ is the transpose of $\ddot{A}$, and $\ddot{A}^{-1}$ is the inverse of $\ddot{A}$.

The added information in the over-determined equations can be used in several ways. Using the estimated atmospheric parameters, estimated return values can be derived and an error [ε] determined from the difference between the actual [S_k] and estimated return values [$S_k^\bullet$]:

$$\varepsilon = \sum (S^\bullet_k - S_k)^2 . \qquad (10)$$

Then this difference can be used to normalize the original geometrical terms:

$$A^\nu_{i,j} = W_i A_{i,j} \qquad (11)$$

where the weight function must be normalized [$\sum_{i'=1}^{I} W_{i'} = 1$], and the tomography equations recalculated using reduced input errors. Another use of the extra degrees of freedom could be to account for

4

temporal changes in the scattering media. For example, the resulting terms might account for changes in optical properties when a constant dry aerosol size distribution is modified by changing humidity.

Computationally, the inversion of the matrix with geometrical terms requires the n^6 multiplications [where n denotes the size of measurement grid] and can not be easily done on small computers except for small grids[4]. However, if the appropriate inverse of the geometrical matrix $[\tilde{A}]$ is calculated ahead of time on a large computer and transferred to a small computer, the number of multiplications is reduced to n^4. Then scattering coefficients can be derived on the PC computer from equation (9). While only two dimensional grids are considered in this report, a three dimensional grid could be analyzed with the same techniques (and such measurements are well within the capabilities of a state-of-the-art lidar).

3. Random Errors and Error Reduction

The tomography analysis technique outlined in section 2 is a 'least squares' process and the errors in the derived parameters matrix are linearly related to the magnitude of errors in the measurement matrix:

$$\vec{B}^\bullet = (\tilde{A}^{-1}\tilde{A}^T)\vec{S}^\bullet, \tag{12}$$

where $\vec{S}^\bullet$ and $\vec{B}^\bullet$ are the errors in the measurement and derived matrices respectively.

To test the sensitivity of this inversion algorithm, a thousand backscatter and extinction matrices were randomly selected with no relationship between backscatter and extinction. The logarithm of the backscatter[β_i] values are selected from a Gaussian distribution with an average of zero and a rms variation of one. The extinction [T_i], which corresponds to the optical depth of each square, are also selected from a Gaussian distribution with an average of 0.1/grid element and a variance that is 10% of the mean value. Using the selected backscatter and extinction, the simulated return values [S] are derived from the original geometrical matrix $[\tilde{A}]$ with a random error [and with a variance of $S^\bullet$] added. Table 2 shows the errors in the extinction and backscatter terms at various grid locations:

$$E_B = \frac{1}{S^\bullet}\sqrt{\frac{1}{I}\sum_{i=1}^{I}(B_i - B_o)^2}, \tag{13}$$

where E_B is the resulting error, I is the total number of observations, and the original input for atmospheric parameters and the output values are B_i and B_o respectively. Except for the last column [j=5], the backscatter errors are moderately larger than the

5

input errors with only a small variation between the various rows and columns. The extinction errors are larger than the backscatter errors and increase in range. Since few returns from the last column are used, the backscatter and extinction errors are substantially larger for this column.

Table 2: Output errors resulting from uniform input errors

		Range [j]					
		1	2	3	4	5	
Distance/ Time [i]	1	1.7 2.5	1.5 5.3	1.4 6.5	2.1 8.1	10.7 17.7	1
	2	1.7 2.4	1.3 5.2	1.4 6.6	1.6 7.6	11.3 24.1	2
	3	1.7 2.5	1.4 5.2	1.4 6.6	1.7 8.2	12.1 21.3	3
	4	1.8 2.5	1.5 5.2	1.4 6.6	1.6 7.8	12.1 23.9	4
	5	1.7 2.5	1.4 5.2	1.4 6.6	2.5 8.0	12.0 20.5	5
		1	2	3	4	5	

Note: Backscatter and extinction errors are respectively on the top and bottom line of each box. Output errors are normalized by input errors.

Table 3 shows analysis of random data when the 'return' [i=0.5,j=3.0] from the center square [i=3.0,j=3.0] has random errors added. While the derived values from the grid with the error are influenced, the least squares process spreads the errors to other squares as well. The last column again has the largest errors and, in the case of extinction, the errors in the center square are not even substantially larger than the other errors in the center column.

Using the derived atmospheric parameters, new 'returns' can be calculated from the geometrical matrix [$\tilde{A}$] and compared with the original 'returns'. For example, in the case discussed above, the difference between derived and original returns was calculated. The recalculated return (from the one which errors were added) has the largest error, which reduces the original error by 80%. Other recalculated returns from the same square [i=0,j=2.5 to i=3.5,j=3.5; i=0,j=3.5 to i=3.5,j=3.5; i=0,j=4.5 to i=3.5,j=3.5; i=0,j=4.0 to i=3.5,j=3.5] increase original error by 10%.

6

Table 3: Output errors resulting from an error to the center square

	Range [j]					
	1	**2**	**3**	**4**	**5**	
1	0.2 0.3	0.1 1.1	2.2 3.8	1.2 10.2	5.1 2.2	**1**
Distance/ **2**	0.4 0.6	0.0 0.2	2.4 4.3	0.4 9.3	6.5 22.8	**2**
Time [i] **3**	1.2 1.9	0.2 2.3	3.4 4.5	1.2 10.9	10.9 8.0	**3**
4	0.4 0.6	0.0 0.2	2.4 4.3	0.4 9.3	6.5 22.8	**4**
5	0.2 0.3	0.1 1.1	2.2 3.8	1.2 10.2	5.1 2.2	**5**
	1	**2**	**3**	**4**	**5**	

Note: Backscatter and extinction errors are respectively on the top and bottom line of each box. Output errors are normalized by input errors and scaled by 10^{-2}.

4. Errors introduced by a changing scattering media

Scattering media can be altered by redistribution of scattering structures and changes in scattering media itself. In this section, changes caused by turbulence to scattering structures are simulated, while the average scattering conditions are left unchanged. Constant movement of the media is not simulated since it is assumed that movement can be removed during the initial analysis of the lidar data.

The spectrum $[F_o]$ of scattering structures is assumed be Gaussian:

$$F_o(\omega_1, \omega_2) = \prod_{i=1}^{2} \frac{\exp[-(\omega_i \sigma_s)^2]}{\sigma_s \sqrt{\pi}} ,$$

where ω is the wave number, the numerical subscript is the grid component, and σ_s is the rms width of the spectrum. Each phase of each Fourier component is selected randomly and has a random phase velocity:

$$F(\omega_1, \omega_2, t) = F_o(\omega_1, \omega_2) \exp\{2\pi i [rnd(\omega_1, \omega_2) + (v_1 + v_2) t]\},$$

where F is the complex magnitude the spectral components, t is time, phase velocities have a gaussian distribution $\exp[-(v_i/\sigma_v)^2]$,

7

and the wave numbers are randomly [$rnd(\omega_1,\omega_2)$] selected. The spectrum with appropriate phases is calculated on a 16 by 16 grid and Fourier transformed with a two dimensional FFT:

$$f(x_1,x_2,t) = \sum_{i=1}^{n}\sum_{j=1}^{n} \exp[-2\pi i\omega_1 x_1/n]\exp[-2\pi i\omega_2 x_2/n]\,F(\omega_1,\omega_2,t),$$

where f is magnitude of the scattering in the real domain and n is the maximum grid size [16]. The final scattering media is a 5 by 5 sub-element selected from the larger grid. This process is done twice to select matrices for backscatter and matrices for extinction. Figure 2 shows the scattering media in one direction where the change of the aerosols structures in time can be seen.

Using tomography, backscatter and extinction errors are calculated for a hundred cases each with eleven time steps. These errors (relative to the original errors) were dependant on the ratio of backscatter to extinction, the dominant structure size, and the rms wind variation of the relative structures. Figure 3 shows the backscatter and extinction errors for the different ratios of these parameters. The smallest errors occur when the ratio is approximately one. When the extinction values are small, the error in the backscatter values are small even when extinction errors are large. Since the extinction is dependant on both backscatter and extinction, this parameter is strongly dependant on both and the error is a minimum when the two errors are comparable in size.
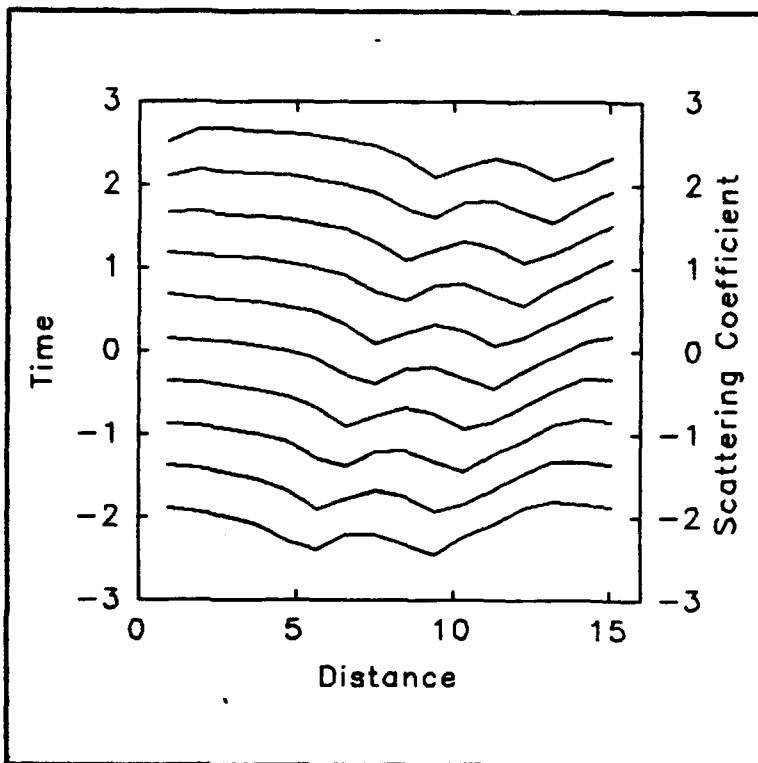

Figure 2: The changes in a typical simulated scattering media are shown. Each line shows the scattering in the one direction through the grid at one time. The different fourier components have different phase velocities which are selected from a Gaussian distribution where the rms variation equals one grid square per each time element.
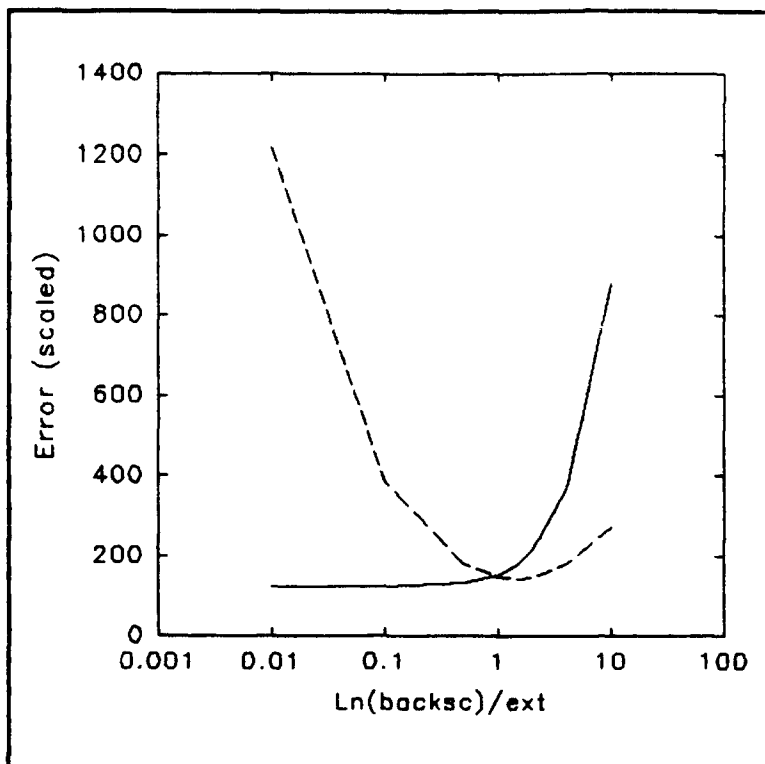
Figure 3: The error scaled for random movement and structure size ($\sigma_u\sqrt{\sigma_s}$) is plotted on the ordinate for the different ratios of backscatter (natural logarithm) and extinction. The extinction and backscatter errors are plotted as solid and dashed lines respectively. Note, the smallest error occurs when the ratio is approximately one.

The relative errors are influenced by the random movement of and the size of the structures. When the structures move rapidly, the scattering media changes quickly and the variation of the scattering media over the measurement cycle becomes larger. Since the smaller structures move a larger fraction of their scale size in shorter time intervals, the relative errors are also dependant on structure sizes. When the backscatter to extinction ratio is one, the relative errors are:

$$\left.\begin{matrix}\beta_{err}\\\sigma_{err}\end{matrix}\right\} = \frac{152}{\sigma_u\sqrt{\sigma_s}},$$

where β_{err} and σ_{err} are the average backscatter and extinction errors divided by the average parameter value, σ_u is the rms variation of speed [in units of one grid dimension divide by one time step], and σ_s is the rms scale size of aerosol structures [in units of one grid dimension].

If each grid element is assumed to be 10 m on a side and random movement of structures is assumed to be 1 m/s, the error for various lidar configurations can be calculated. For an aircraft moving at 100 m/s over a media which has a dominant structure size of 1 km, the relative error becomes 15%, which is acceptable for many atmospheric measurements. For a stationary lidar when the wind speed is 10m/s, the error is 150% which is not acceptable.

5. Summary and Conclusions

Tomography can be used to simultaneously measure both backscatter and extinction measurements. However, the method is limited. The scattering properties need to be almost homogenous inside the tomography grid elements and must not change significantly during the measurement cycle. Computationally the most multiplications required is n^6. With a pre-calculated inverted geometrical matrix $[\tilde{A}]$, the solution of individual terms requires n^4 multiplications.

Since the equations are over-determined, scattering properties can be derived from a least squares fitting process. Errors are linearly related to the matrix relationship, which includes linear extinction and logarithmic backscatter terms. The technique is, in theory, not limited to two dimensional cases, but can be used for three dimensional grids as well.

Unlike some lidar inversion processes, the tomography method is not limited to a fixed backscatter to extinction relationship. This is especially important for environmental conditions (such as coast lines) where the aerosols change on short spatial and temporal scales.

All the analysis was done for a single flat scanning scheme where the lidar is scanned $\pm 45°$ perpendicular to the average wind. This scheme is achievable with many existing scanning lidars, and while no effort was made to find the optimal scanning scheme to minimize errors, wider scanning angles should reduce errors.

The sensitivity of this algorithm to random movement restricts the tomographic applications of single stationary lidars. For accurate detailed analysis, multiple spatially separated lidars will probably be needed. With two scanning lidars, the unknowns match the number of observations and, while the inversion is possible, the errors would be large, since the errors for each observation can not be reduced by a least squares fitting process. However, with three lidars, a suitable inversion should be possible, since the scattering media can be characterized from an over-determined set of equations.

10

References:

1.   R. M. Measures, <u>Laser remote sensing: fundamentals and applications</u>, Wiley & Son, New York (1984).

2. J.A. Weinman,"Tomographic lidar to measure the extinction of atmospheric aerosols"Appl Opt 23,3882-3888(1984).

3. L.W.Johnson and R.D. Riess,"Numerical Analysis,"Addison-Wesley, Reading, Ma,1977.

4. The number of multiplications represents a worst case scenario and, since the matrix has many zeros, more efficient algorithms designed for sparse matrices may reduce the number of required multiplications.